Manuscript No: JBC/2009/096354

Supplementary Data

The CPVT mutation R33Q disrupts the N-terminus structural motif that regulates reversible calsequestrin polymerization

Naresh C. Bal, Ashoke Sharon, Subash C. Gupta, Nivedita Jena, Sana Shaikh, Sandor Gyorke and Muthu Periasamy*

LEGENDS TO SUPPLEMENTARY FIGURES

Figure S1. Multiple Sequence alignment of calsequestrin from residue 60 to C-terminus. There are dispersed patches of highly conserved residues throughout the molecule, which might be important for Ca^{2+} buffering and dynamic polymerization and depolymerization. The labeling is same as in the figure 1 in the text. Accession numbers are as follows: NP_001133632 (*Salmo*, Atlantic salmon), CAG00977 (*Tetradon*), NP_001002682 (*Danio*, zebrafish), BAG49513 (*Solea*, Senegalese sole), AAH80039 (*Xenopus*, Western clawed frog), NP_033944 (*Mus*), NP_058827 (*Rattus*), NP_001223 (*Homo*), XP_513677 (*Pan*, chimpanzee), Q5RAN9 (*Pongo*, orangutan), XP_001101353 (*Macaca*), NP_001095161 (*Oryctolagus*), NP_001030451 (*Bos*), XP_001500410 (*Eqqus*), XP_001363916 (*Monodelphis*, opossum), NP_989857 (*Gallus*), NP_033943 (*Mus* CASQ1), NP_001222 (*Homo* CASQ1), XP_002130664 (*Ciona*, sea squirt), and XP_001677823 (*Caenorhabditis*).

Figure S2. Conformation of CASQ2 mutants at 0 mM $CaCl_2$. Far UV CD spectra of cluster #1 **(A)** and cluster #2 **(B)** mutants. None of the mutations affected conformation of the protein in absence of Ca, the concentration at which these proteins are expected to be present predominantly in monomeric state. Hence these point mutations had no effect on protein conformation at monomeric level.

Figure S3. Thermal stability of CASQ2 mutants. Far UV CD spectra of cluster #1 **(A)** and cluster #2 **(B)** mutants at temperatures indicated in °C. Mutants of Cluster #1 behave more like R33Q mutant while cluster #2 mutants behave more like WT protein. This suggests that cluster #1, which is highly conserved, is indispensable for Ca^{2+}-induced CASQ2 polymerization (supported by figure 3 in text and S3 below); while cluster #2 is dispensable and it is less conserved in evolution.

Figure S4. Ca^{2+}/EGTA-induced structural changes as analyzed by CD spectra (A) cluster #1 mutants; Charge alteration in cluster #1 leads to loss of reversible polymerization. **(B) Cluster #2 mutants**; Single charge neutralization of cluster #2 'E39A' could not affect polymerization-depolymerization behavior. In contrast, double charge neutralization of cluster #2 'K40A-K43A' shows altered CD spectra in presence of 5 mM $CaCl_2$, effect was intermediate between WT and R33Q. Interestingly however, K40A-K43A could regain native conformation upon Ca^{2+}-chelation with EGTA.

Figure S5. Polymerization dynamics of WT and mutant CASQ2 as analyzed by turbidimetric assay: As shown in figure 3C and 3D, WT-CASQ2 can undergo rapid aggregation and resolubilization at physiological [Ca^{2+}] (~2.0 mM) and at ~2.5 mM EGTA concentration respectively. However, mutations in cluster #1 alter this bidirectional transition. Replotting of data from figure 3 reveals Ca^{2+}/EGTA mediated transition of WT **(A)**, R33Q **(B)**, D29A-D32A **(C)**, and K31A-K33A **(D)**. The percentage of protein aggregate at 0 mM EGTA is highest before EGTA mediated chelation. The calcium induced aggregation and disaggregation (by EGTA) curve for the WT protein is qualitatively similar to the mathematical calculation by Restrepo et al, 2008. However, mutation in the crucial cluster #1 shifts the transition to the right deterring buffering-polymerization dynamics.

Manuscript No: JBC/2009/096354

Supplementary Figures

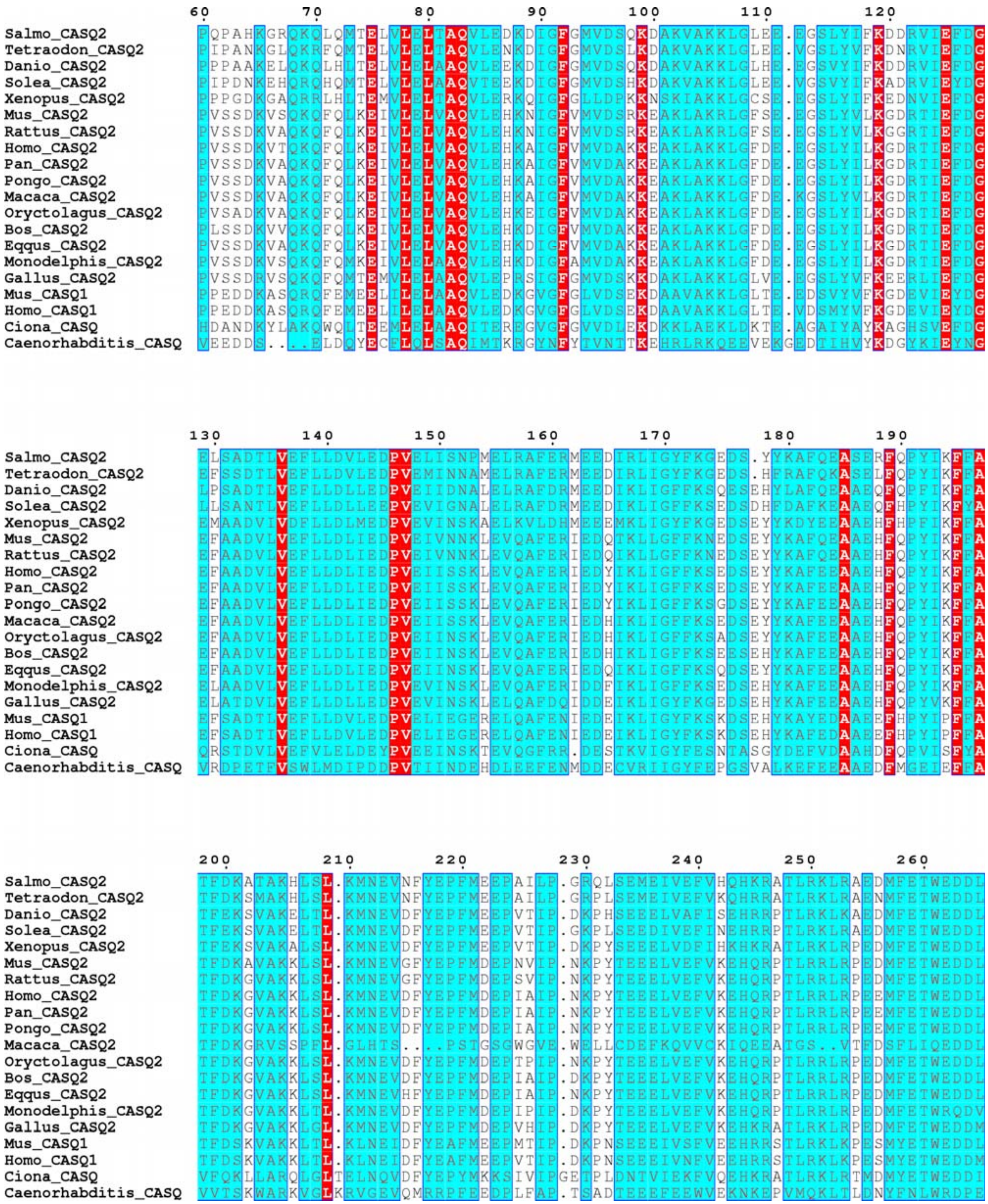

Figure S1

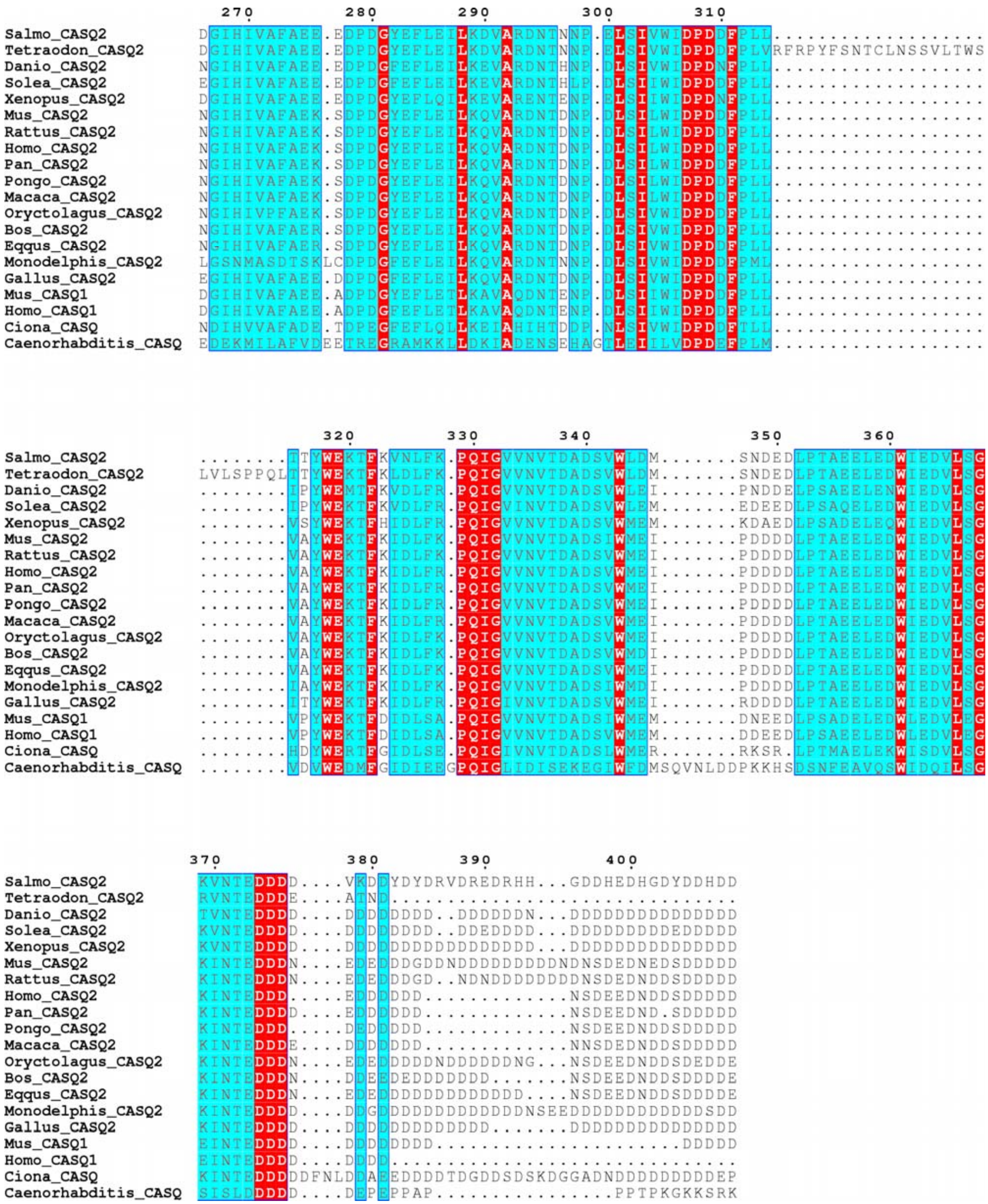

Figure S1 continued

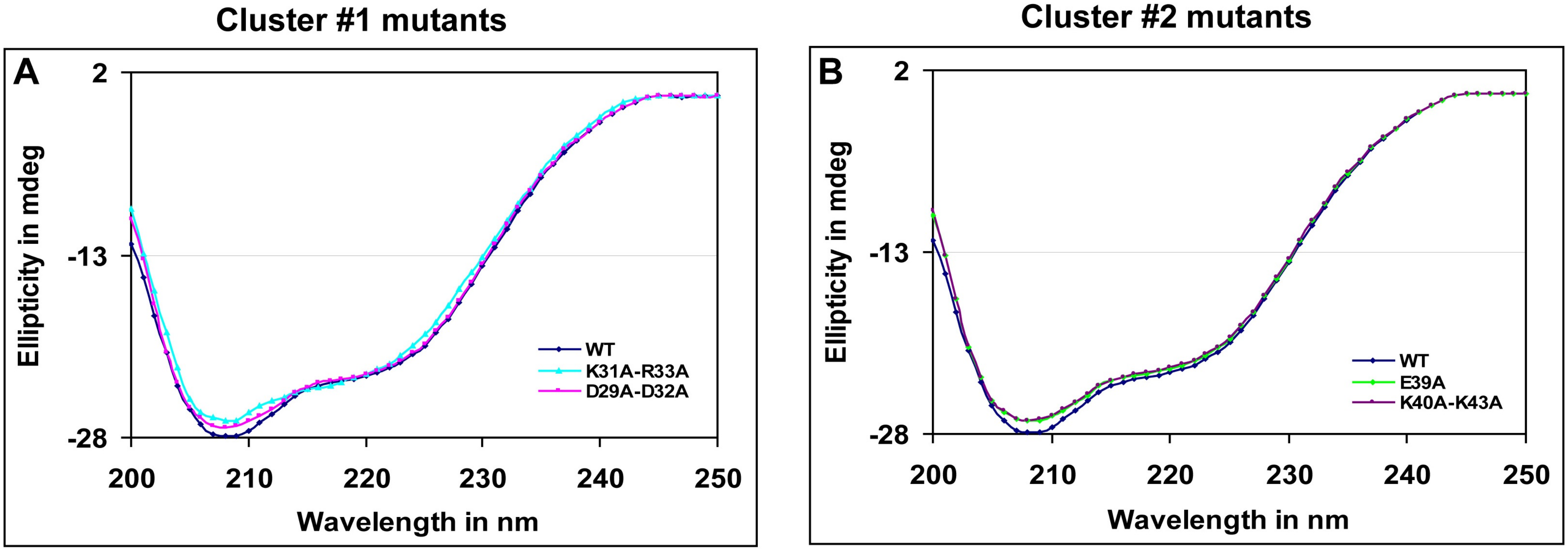
Cluster #1 mutants
A
Ellipticity in mdeg
2
-13
-28
200
210
220
230
240
250
Wavelength in nm
WT
K31A-R33A
D29A-D32A
Cluster #2 mutants
B
Ellipticity in mdeg
2
-13
-28
200
210
220
230
240
250
Wavelength in nm
WT
E39A
K40A-K43A

Figure S2

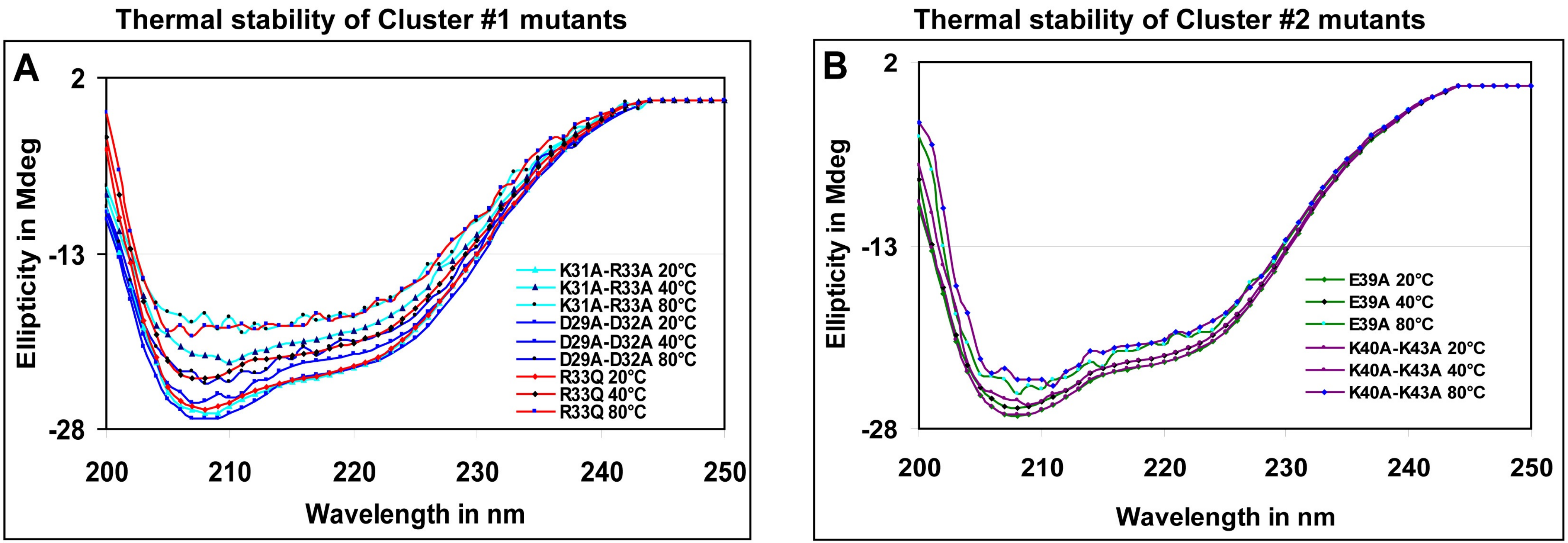

Thermal stability of Cluster #1 mutants
A
2
-13
-28
Ellipticity in Mdeg
200
210
220
230
240
250
Wavelength in nm
K31A-R33A 20°C
K31A-R33A 40°C
K31A-R33A 80°C
D29A-D32A 20°C
D29A-D32A 40°C
D29A-D32A 80°C
R33Q 20°C
R33Q 40°C
R33Q 80°C
Thermal stability of Cluster #2 mutants
B
2
-13
-28
Ellipticity in Mdeg
200
210
220
230
240
250
Wavelength in nm
E39A 20°C
E39A 40°C
E39A 80°C
K40A-K43A 20°C
K40A-K43A 40°C
K40A-K43A 80°C

Figure S3

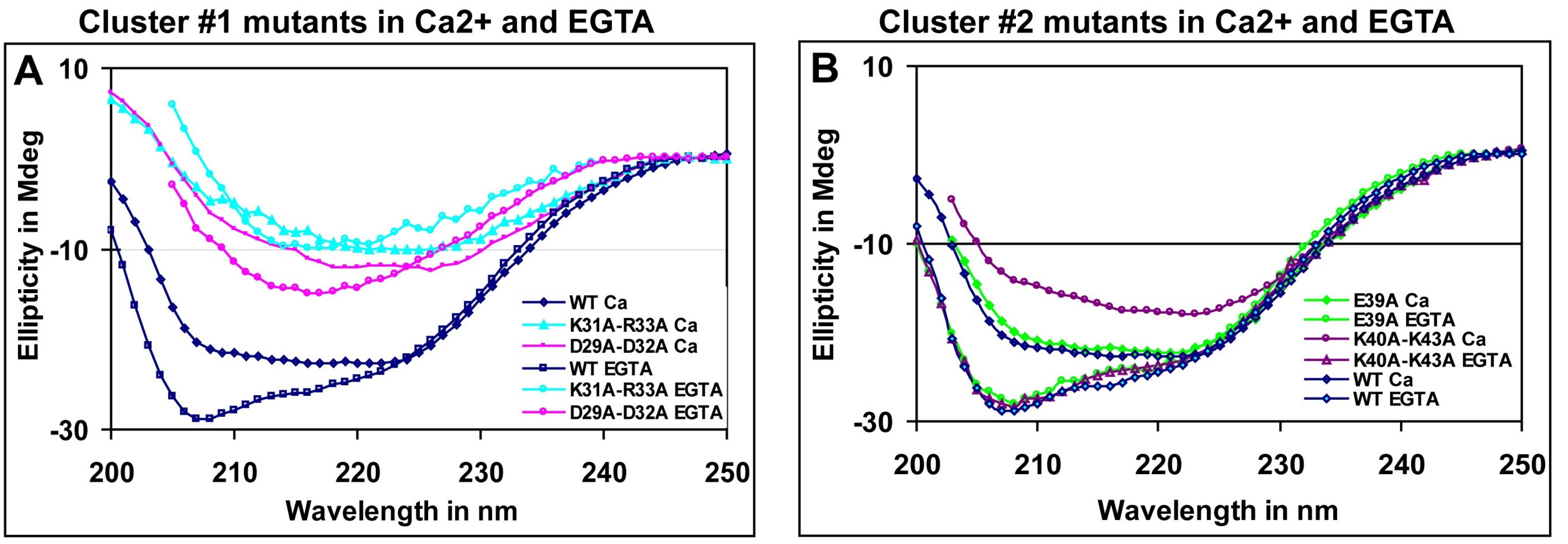

Cluster #1 mutants in Ca2+ and EGTA
A
10
-10
-30
Ellipticity in Mdeg
200
210
220
230
240
250
Wavelength in nm
WT Ca
K31A-R33A Ca
D29A-D32A Ca
WT EGTA
K31A-R33A EGTA
D29A-D32A EGTA
Cluster #2 mutants in Ca2+ and EGTA
B
E39A Ca
E39A EGTA
K40A-K43A Ca
K40A-K43A EGTA
WT Ca
WT EGTA

Figure S4

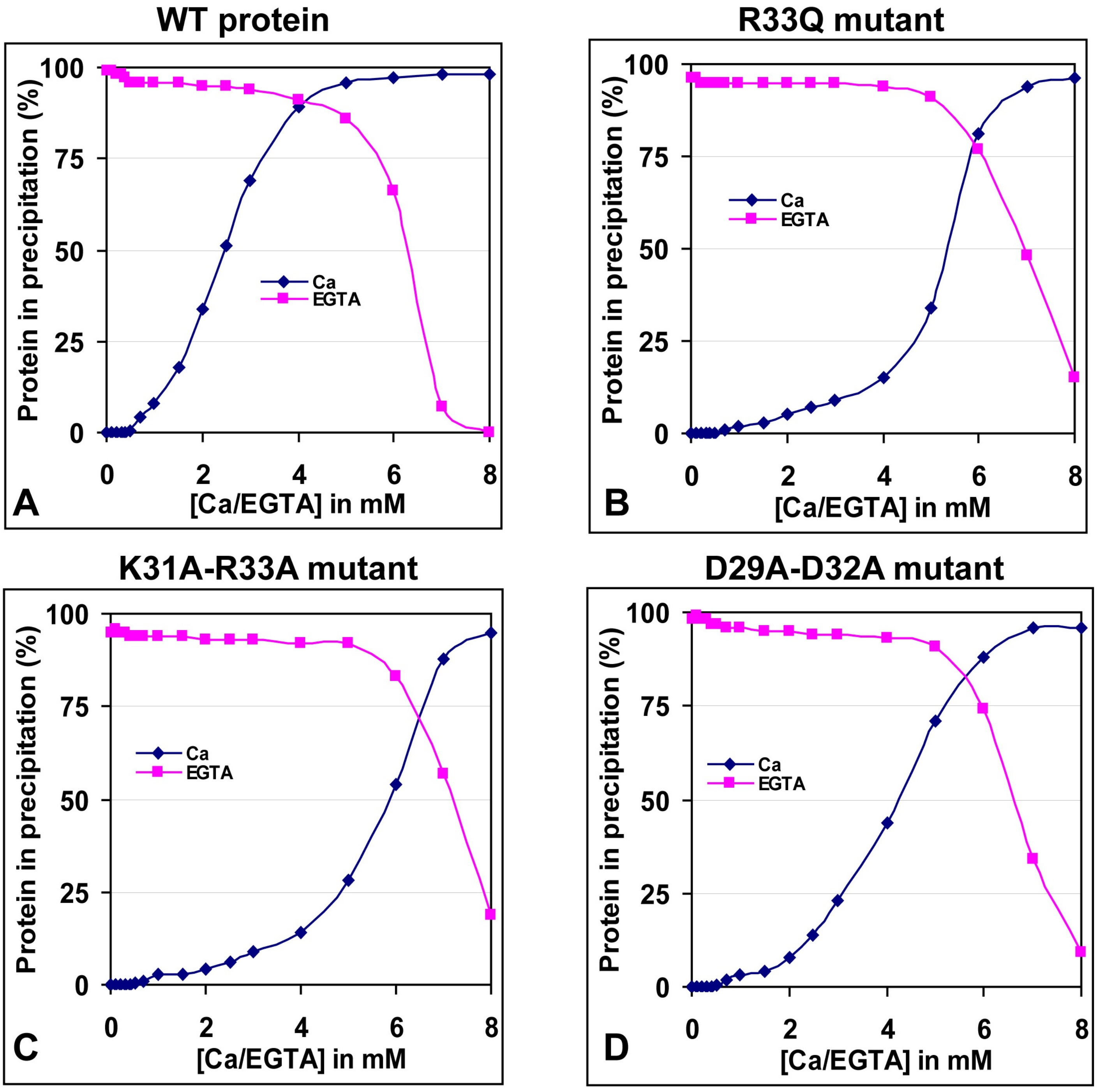
WT protein
R33Q mutant
K31A-R33A mutant
D29A-D32A mutant
Protein in precipitation (%)
[Ca/EGTA] in mM
Ca
EGTA
0
25
50
75
100
2
4
6
8
A
B
C
D

Figure S5